New Jersey Geological Survey
Technical Memorandum TM 89-2

DETERMINATION OF BEDROCK TOPOGRAPHY AND GEOLOGY USING VARIOUS GEOPHYSICAL TECHNIQUES

Department of Environmental Protection
Division of Water Resources

1989

STATE OF NEW JERSEY
Thomas H. Kean, *Governor*

Department of Environmental Protection
Christopher J. Daggett, *Commissioner*

Division of Water Resources
Eric Evenson, *Acting Director*

Geological Survey
Haig F. Kasabach, *State Geologist*

New Jersey Geological Survey
Technical Memoranum TM 89-2

DETERMINATION OF BEDROCK TOPOGRAPHY AND GEOLOGY USING VARIOUS GEOPHYSICAL TECHNIQUES

by
Suhas L. Ghatge, David L. Pasicznyk, Stewart K. Sandberg,
David W. Hall, and John C. Groenewold

New Jersey Department of Environmental Protection
Division of Water Resources
Geological Survey
Trenton, NJ 08625

1989

New Jersey Geological Survey technical memorandums are brief reports prepared for timely response to issues of concern. This report may be quoted provided that the following format is used:

> Quoted excerpt (in quotation marks), New Jersey Geological Survey Technical Memorandum 89-2, Ghatge and others, 1989.

CONTENTS

page
Abstract. 1
Introduction. 1
Acknowledgements. 2
Geology. 2
Geophysical Field methods. 3
Seismic 3
Electrical Resistivity-Induced Polarization. 4
Electromagnetics 4
Microgravity 5
Magnetics. 5
BoreholeGeophysics. 5
Geophysical Data reduction and interpretation. 5
Seismic Refraction. 5
Electrical Resistivity-Induced Polarization. 5
Electromagnetics. 8
Microgravity. 15
Magnetics. 15
Borehole Geophysics. 19
Conclusions. 19
References. 21

FIGURES

page
Figure 1. Location and topography of study area. 2
2.Pre-Quatemary geology and location of wells 3
3. Seismic refraction travel-time curves" "
a. 2O-foot geophone-interval data. 6
b. SO-foot geophone-interval data. 6
4. Interpreted seismic refraction depth section. 7
5 a. Schlumberger sounding resistivity and induced-polarization curves (MCVES 5) and interpretation. 9
b. Schlumberger sounding resistivity and induced-polarization curves (MCVES 7) and interpretation. 10
c. Schlumberger sounding resistivity and induced-polarization curves (MCVES 6) and interpretation. 11
6 a. Transient electromagnetic curves MCTEM3, MCTEM4 and MCTEM5 12
b. Pseudosection plot of TEM soundings MCTEM3, MCTEM4 and MCTEM5 12
c. Linear plot of field data from TEM sounding MCTEM3 12
d. Schlumberger resistivity sounding MCVES 7 with TEM sounding MCTEM1 and interpretation. 13
e. Terrain-conductivity profile data. 14
7. Residual gravity profile and interpretative model, showing density contrasts. 16
8. Total magnetic field intensity profile and interpretative model, showing modeled bodies and their associated magnetic susceptibilities. 17
9. Natural gamma log, single-point resistance log and borehole lithologic log. 19
10. Composite bedrock and overburden profile. 20

APPENDIX

page
Records of wells 23

DETERMINATION OF BEDROCK TOPOGRAPHY AND GEOLOGY USING VARIOUS GEOPHYSICAL TECHNIQUES

by
Suhas L. Ghatge, David L. Pasicznyk, Stewart K. Sandberg,
David W. Hall and John C. Groenewold

ABSTRACT

To test the effectiveness of differing geophysical techniques alone and in combination, various surface and borehole geophysical techniques were used to determine bedrock topography and geologic characteristics of the overburden in Central Mercer County Park, New Jersey. The surface geophysical methods were seismic refraction, electrical resistivity, induced polarization (IP), electromagnetics (transient and frequency-domain), microgravity, and magnetics. The borehole geophysical methods were-natural gamma and single point resistance logging. Lithologic descriptions from nearby wells and a borehole drilled on-site were used as an independent check on results.

Seismic refraction was successful in determining depths to bedrock and the water table. Electrical and electromagnetic soundings were useful in determining lithology of near-surface and deeper-lying unconsolidated deposits and bedrock along a 1640-ft-Iong profile. Depth to bedrock from seismic interpretations was used to constrain the gravity and magnetic interpretations. The combined interpretations indicate an undulating bedrock surface. Magnetic anomalies may reflect either variations in susceptibility within the bedrock or complex folding of units of differing susceptibility.

A composite profile comparing interpretations of bedrock topography based on each geophysical method shows close agreement between methods and between geophysical interpretations and the borehole log. Variations of physical properties of the bedrock and overlying sediments, together with limitations of the different geophysical methods, led to slight differences in interpreted bedrock depths.

INTRODUCTION

In 1985, 1986 and 1987 the New Jersey Geological Survey conducted geophysical investigations to examine the effectiveness of various surface and borehole geophysical techniques in determining depth to ground water, depth to bedrock, and lithology of bedrock and overlying sediments and to evaluate how the methods may be used in combination to obtain more information than can be obtained using them separately.

The investigation was carried out along a 1640-ft-longprofile on an unpaved road north of Assunpink Creek in Central Mercer County Park, West Windsor Township, Mercer County, New Jersey (fig. 1). The site was selected because it was free of cultural noise from powerlines, fences, buildings, and so forth, and because it resembles sites of many hydrogeologic investigations in New Jersey in that several tens of feet of unconsolidated sediment and weathered material overlie bedrock.

The different surface geophysical methods used were seismic refraction, electrical resistivity, induced polarization, electromagnetics (transient and frequency-domain), microgravity and magnetics. The borehole geophysical methods were natural gamma and single-point resistance logging. The advantages of using a combination of geophysical methods for ground-water exploration or buried-valley studies has been discussed by Lennox and Carlson (1967), Eaton and Watkins (1970), and van Overmeeren (1981).

The topography of the site is slightly undulatory with elevations ranging from 60 to 100 ft above sea level (fig. 1). The site is approximately 8 miles northeast of Trenton and 4.5 miles south of Princeton. The survey profile is oriented NW-SE and is accessible from Village Road to the north or South Post Road to the east (fig. 1). All measurements along the profile are in feet

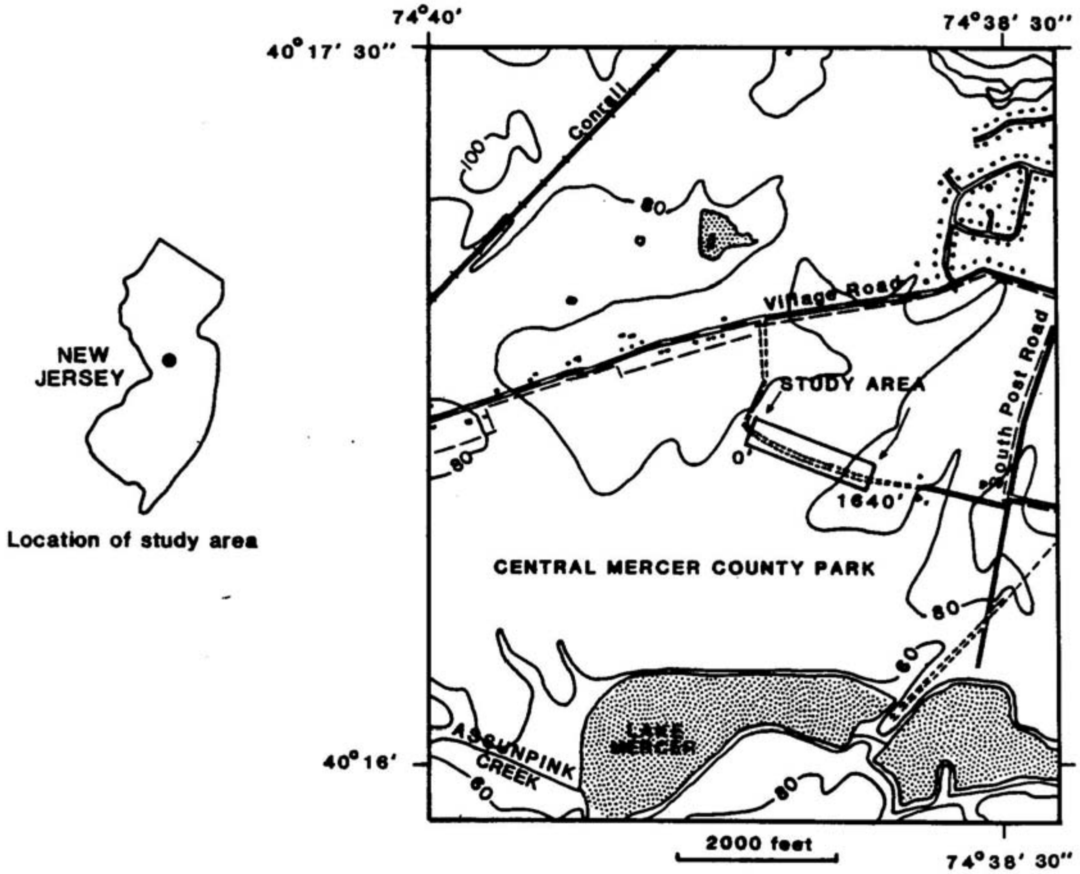

Base map from US Geological Survey, Princeton Quadrangle, 1981.
Contour interval 20 feet.

Figure 1. Location and topography of study area

from 0.0 at the NW terminus to 1640.0 at the SE terminus.

Acknowledgements

The authors thank the Mercer County Park authorities for permitting us to collect data at the site. In addition we thank the following personnel of the New Jersey Geological Survey: Jeffrey Waldner, James Boyle, and Donald Jagel for field and office assistance; Mike Mccullough for drilling; John Curran for geophysical logging and Richard Volkert for lithologic logging. Jeffrey Kearns, Cordelia Pierson and Thomas Bambrick, formerly with the New Jersey Geological Survey, also helped in the data collection.

GEOLOGY

In Mercer County Park surficial sands and gravels of the Pensauken Formation overlie sands, silts and clays of the Raritan and Magothy Formations (Johnson, 1950). These in turn overlie Precambrian or early Paleozoic schists of the Wissahickon Formation and Precambrian granitoid gneisses. Mesozoic sandstone of the Stockton Formation is exposed to the northwest (fig. 2). Bedrock lithology near the centerline of the profde is known from a borehole (no. 9 of fig. 2) completed after interprtation of the geophysical data. The log shows unconsolidatedsediments to a depth of 75 ft, weathered bedrock (saprolite) to 128 ft, granitic rock to 138 ft, gneiss

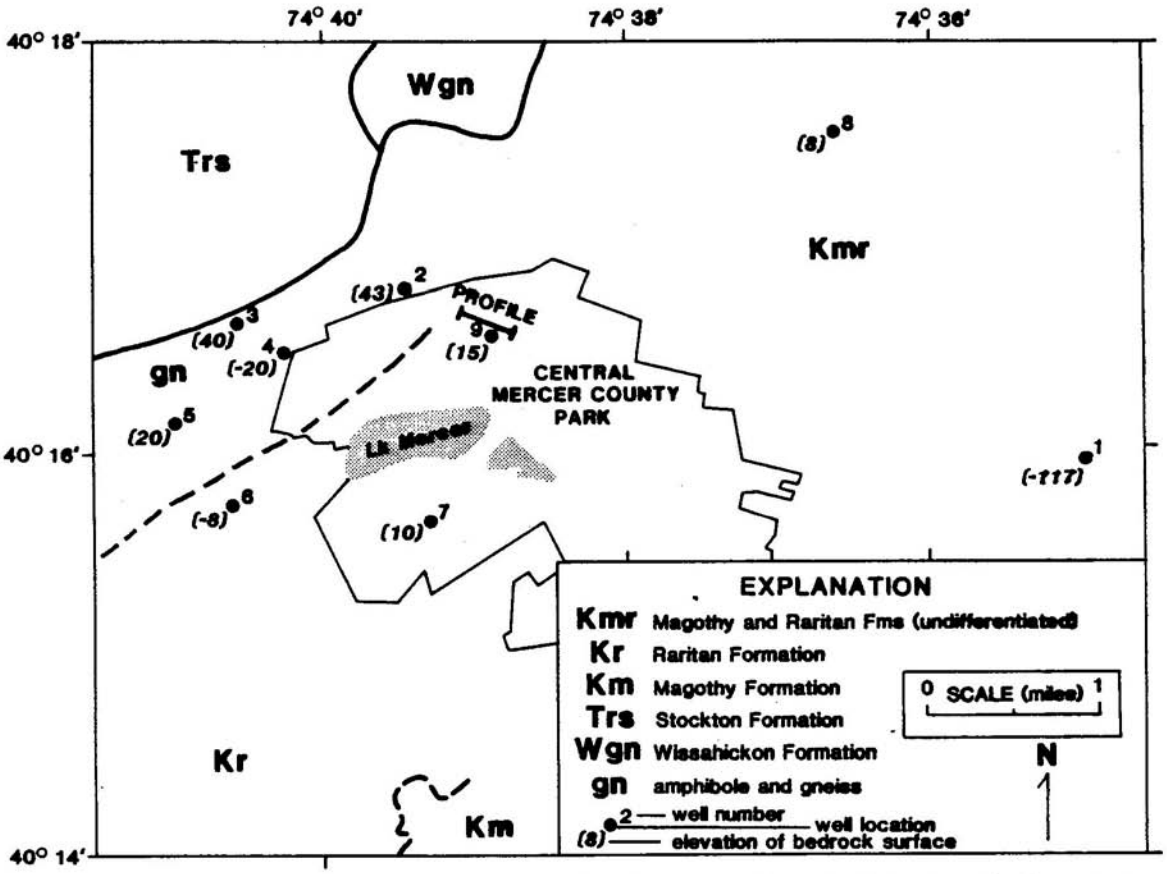

Modified from New Jersey Geological Survey, Geologic Atlas, Sheet 28 overlay, scale 1:63,360, undated, ca. 1965

Figure 2. Pre-Quaternary geology and location of wells.

to 213 ft, alaskite to 224 ft, an altered mafic rock to 258 ft and gneiss again to the total depth of the borehole at 270 ft (Richard Volkert, NJ. Geological Survey, written communication, 1987). Drillers logs (appendix) show sand, gravel and clay overlying granitic or gneissic bedrock in the vicinity of the profile.

Regional slope of the bedrock surface is several feet per mile to the southeast (Widmer, 1965). On a local scale, however, a subdued, undulatory topography is more apparent (fig. 2). Well records show the bedrock surface at 43 ft below sea level 0.47 mile west of the survey line and 117 ft below sea level 3.3 miles east of the line. Wells to the north and south of the line encountered bedrock at shallower depths.

GEOPHYSICAL FIELD METHODS

Seismic Refraction

Seismic data were recorded on a 12-channel, non-saturating, signal enhancement seismograph (Bison GEOPRO Model 8012A). Analog filter settings of 35Hz high pass and 100 Hz low pass were used. A single feedback-sensitive accelerometer (Terra Dynamics ADR 711) per trace was used throughout the survey.

The data were collected at two different times, using different geophone station intervals.

Initially, a 20-ft geophone interval was used with maximum shotpoint offsets of 200 ft, yielding data from relatively shallow depths. Subsequent interpretation of resistivity-induced polarization data indicated a deeper high-resistivity layer. Consequently, more data were collected using a 5O-ft geophone spacing with a maximum shotpoint offset of 550 ft.

The seismic source used with the 20-ft geophone spacing data was a "Buffalo Gun" (a device used to detonate an 8-, 10- or 12- gauge shotgun shell in a fluid-filled borehole). The 20-ft geophone data were collected along a linear profile composed of seven spreads, twelve geophone stations per spread. Two reversed profiles were taken at each geophone spread, one pair with the sources at the ends of the spread and another with the sources offset 200 ft from the end geophones. The first geophone of successive spreads maintained the geophone interval of 20 ft.

A vacuum-assisted weight drop (EG&G Dynasource) was used as the source for the 50-ft geophone spacing data. Three continuous geophone spreads, twelve geophone stations per spread were completed. The spreads consisted. of reversed profiles, profiles offset 550 ft and split profiles in which the shotpoint was at the midpoint of the spread.

Electrical Resistivity and Induced Polarization

Three electrical resistivity and induced polarization soundings were made on the site. These soundings were centered at the 328.1-ft, 820.2-ft and 1312.3-ft marks. These soundings are referred to as MCVES5, MCVES7 and MCVES6.

Resistivity and induced polarization data were taken in the Schlumberger array. Data were obtained using the Huntec M4 2.5-kW induced polarization system manufactured by Huntec Ltd., Toronto, Canada. Copper-copper sulfate porous pot electrodes were used at the receiver for the voltage measurements, and stainless steel stakes were used for transmitting current into the ground. The data were recorded on digital cassette tapes.

The data were collected in the time domain from a transmitted waveform composed of alternating two-second segments of on-positive, off, on-negative, and off pulses. Voltage readings at the receiver were obtained during the on-time and for ten windows of 100-ms width starting 100 ms after turnoff of the transmitted current. The on-time voltage measurements were used to calculate the apparent-resistivity data. The induced polarization data consisted of apparent chargeabilities which were calculated by summing the integrals of the voltage over each of the time windows and then dividing this sum by the average on-time voltage, resulting in units of milliseconds (ms).

Electromagnetics

Electromagnetic depth-sounding and profiling were both performed at the test area. A transient electromagnetic (TEM) method was used in the "in-loop sounding" (or central loop sounding) configuration, and a frequency-domain (terrain conductivity) electromagnetic method was used to profile in the "horizontal loop" configuration.

TEM data were collected using Geonics EM-37 equipment, which is one of the more common TEM systems. The "in-loop sounding" configuration consists of a square horizontal transmitting loop with a receiver coil positioned at the center of the loop in a coaxial mode. Current is driven in the transmitting loop in a modified square wave at a 3Q-Hz transmitting frequency, current is on-positive, off, on-negative, off, on positive again, and so forth with equal intervals of 1J120th of a second. The vertical magnetic field induced in the receiver coil is sampled at logarithmically-spaced time intervals after the transmitter current is shut off. Data are then stacked to decrease the effect of random noise.

Four TEM sounding sites were occupied in the survey area. The first site (MCTEM1) was centered at 942 ft, the second (MCTEM3) was centered at 1483 ft, the third (MCTEM4) was centered at 1319 ft, and the fourth (MCTEM5) was centered at 1152 ft. The transmitters were square loops with side lengths of 984.3 ft for MCTEM1, and 246 ft for the other three soundings.

Terrain conductivity measurements were collected along the entire study profile using the Geonics EM-34-3 electromagnetic system. Data were taken in the horizontal loop (vertical dipole, coplanar) configuration at a constant separation between transmitter and receiver of 131.2 ft, and a station spacing of 16.4 ft. Measurements consist of apparent conductivity of the ground at each station.

Microgravity

The Lacoste & Romberg Microgal Gravity Meter (Model # D25) capable of being read to the nearest 0.001 milligal (mGal, 1 mGal = 0.001cm/sec^2) was used in this study. Gravity readings were taken along the survey line at 82.0-ft intervals. Accuracy of the gravity meter readings was maintained by taking repeated observations at each station until duplication was obtained within 0.02 of the dial reading. Counter readings were converted to mGal values by using the gravity-meter specifications for conversion. Station elevations were obtained by rod-andlevel surveying with an accuracy within $\pm$0.2 ft.

The primary base station, established by Princeton University (Bonini and Woollard, 1957), is in the center of the corridor between rooms 13 and 15 in the old part of Guyot Hall, Princeton University, Princeton, New Jersey. The observed gravity at this station is 980177.6 mGals. The secondary base station was established at the 1640.0-ft mark at the eastern end of the profile (fig. 1) by tying it with the primary base station at Princeton University.

Magnetics

Magnetic data acquisition was conducted using an EG&G Geometrics G-856 Proton Precession Magnetometer. This instrument measures the earth's total magnetic field with a resolution of 0.1 gamma and an accuracy of 0.5 gamma.

Magnetometer readings were taken along the profile at 82.0-ft intervals. To compensate for diurnal variations of the Earth's magnetic field, readings were repeated every 1.5 hours at a base location established at the site.

Borehole geophysics

A WIDCO (model 1200) single-conductor analog well logger was used to collect borehole geophysical data at borehole 9 (fig. 2), drilled for this study at the 900-ft position along the profile. Natural gamma and single-point resistance logs were run in the 4-inch-diameter borehole. The single-point resistance tool was operated only below 128 ft because the borehole was cased to this depth.

GEOPHYSICAL DATA REDUCTION AND INTERPRETATION

Seismic Refraction

The seismic data were reduced and interpreted using microcomputer-based processing. Arrival times for the seismic events (fig. 3) and the corresponding layer numbers were calculated using HRASSD (Hoffman and Waldner, 1985), an interactive seismic-processing computer program. The arrival times and representative layer values were used as input for a seismic-refraction inverse-modeling computer program, SIPT (Scott and others, 1972; Scott, 1977). The SIPT program is based on the delaytime method and a ray-tracing modeling technique from which calculated average velocities were used to generate depth sections.

Refraction data sets from the 20- and 50-ft geophone spacings were interpreted separately because of computer software limitations. Resolution of the upper layers is severely limited with the 50-ft geophone spacing. This is to be expected inasmuch as data taken with the 20-ft spacing has more than twice as many ray-end points as that taken with a 50-ft-spacing data. The crossover points of the 50- ft geophone interval traveltime curves are ambiguous. The only real discrepancy between the two models is at this interface. Aliasing due to the large sample interval and the crossover point ambiguity account for this. Calculated layer velocities for each spread indicated fairly uniform velocity within each layer through the entire profile.

Interpreted results of the two data sets (fig. 4) indicated four layers. The first layer, a nearsurface unsaturated sand and gravel, had an average velocity of 2,030 ft/sec The second layer, a saturated sand and gravel, had an average velocity of 5,600 ft/sec While the third layer, most likely weathered crystalline rock, had an average velocity of 14,900 ft/sec and the fourth layer, most likely unweathered crystalline rock, had an average velocity of 20,600 ft/sec.

Electrical resistivity and induced polarization

The electrical resistivity and induced-polarization (IP) data were reduced to apparent resistivities. The modeling consisted of fitting a horizontally stratified earth model to both the resistivity and IP data simultaneously using a non-linear, least-squares inversion program, IPINV (John Groenewold, formerly of NJ. Geological Survey, written communication, 1986) incorporating the Marquardt procedure

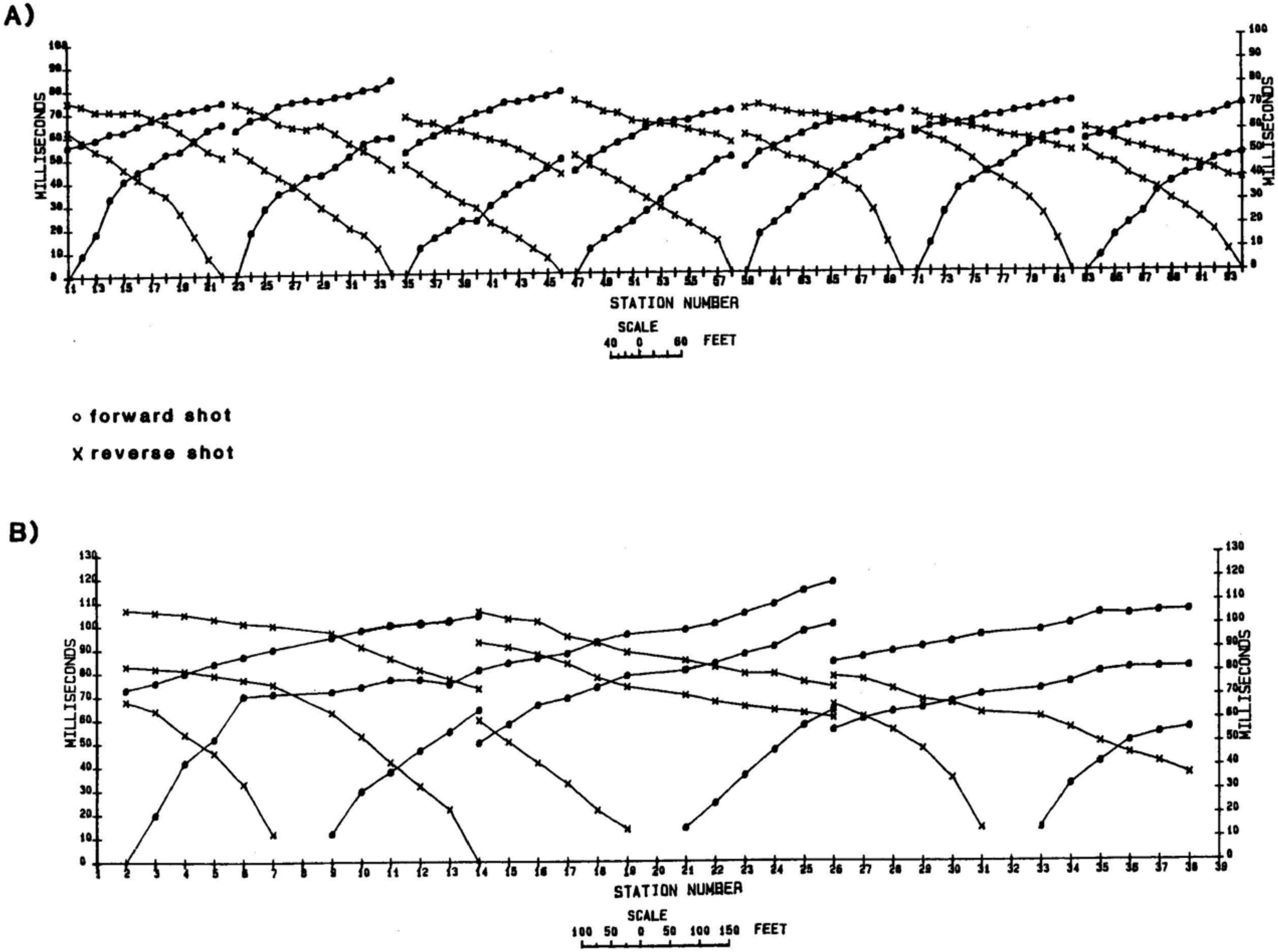

Figure 3. Seismic refraction travel-time curves. *a.* 20-foot geophone interval. *b.* 50-foot geophone interval.

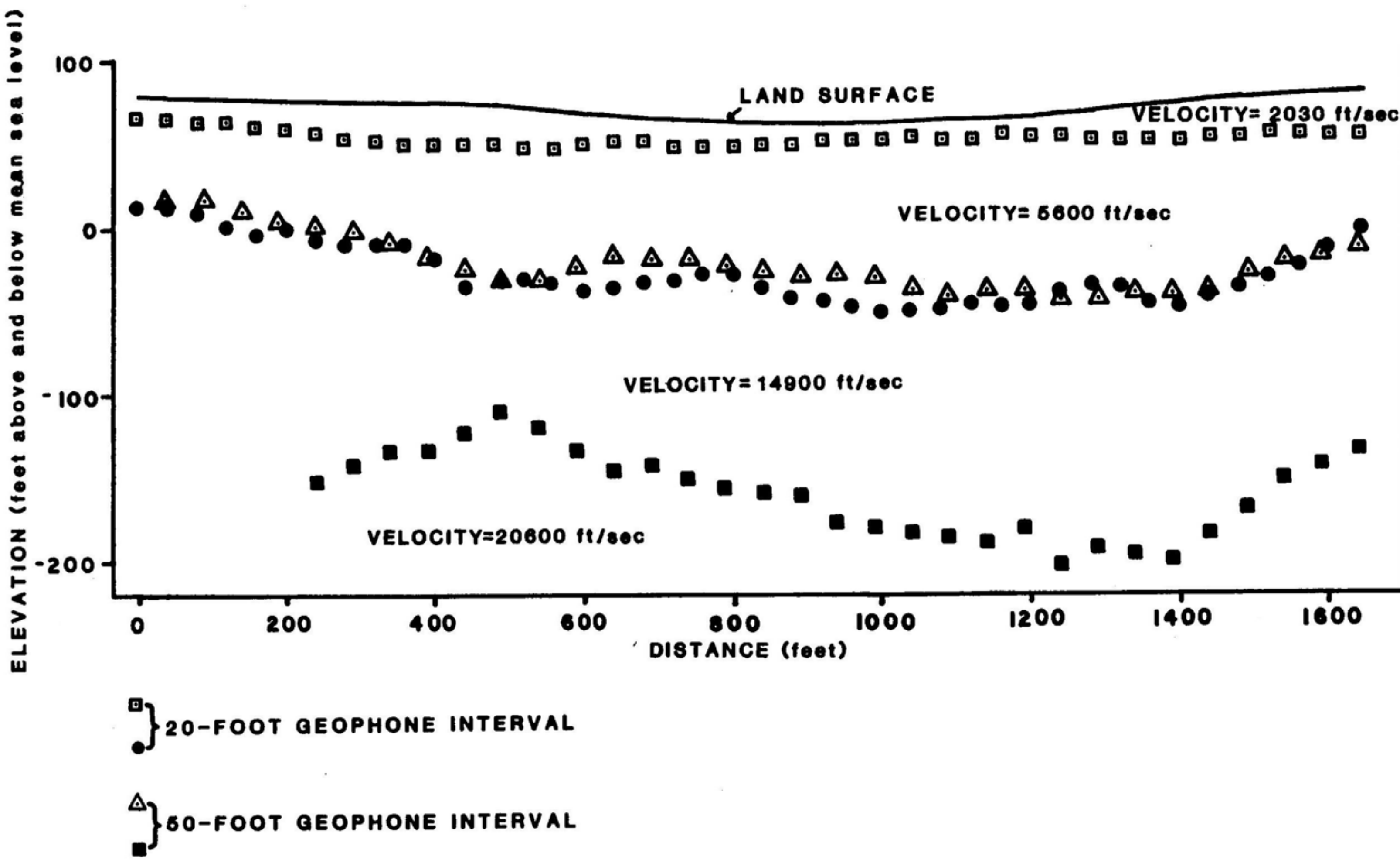

Figure 4. Interpreted seismic refraction depth section.

(Beck and Arnold, 1977). The forward routine used in the inversion program is based on the convolution method presented by Koefoed (1972).

The interpreted results of the three Schlumberger soundings, MCVES5 (fig. 5a), MCVES7 (fig. Sb) and MCVES6 (fig. 5c), indicate four principal layers above the weathered bedrock. The layering sequence as determined from the resistivity and IP data is much the same as from the seismic model. Layers one and two are silty sand with clay concentration increasing with depth as evidenced by the increase in chargeability from layer one to layer two. The resistivity of the third layer is typical of saturated sand, and the high chargeabilities indicate the possible presence of clay. The low resistivity and chargeability of the fourth layer corresponds to the properties expected of the saprolite (weathered material) at the top of bedrock. The resistivity of the fifth layer (or basal half space) is very high, indicating that this layer is the crystalline basement. The resistivity of the fifth layer was poorly resolved, typically displaying the largest percent standard deviation of all the model parameters.

Electromagnetics

TEM measurements consist of voltages induced in a receiver coil. These are converted to apparent resistivity as a function of measurement time. Apparent resistivity calculations were performed by the computer program RAMPRES (Sandberg, 1988). Variables used in the calculation include magnitude of the transmitted current, effective area of the receiver coil, size of the transmitting loop, and shut -off time of the current ramp. RAMPRES normalizes the effects of changes in these variables, and also converts from voltage readings, which can range over 5 orders of magnitude, to resistivities, which have clearer physical signifIcance and smaller range.

A plot of apparent resistivity versus time for soundings MCTEM3, MCTEM4 and MCTEM5 is shown in figure 6a. Qualitatively, "early time" corresponds to shallow strata and "late time" corresponds to deeper strata. As can be seen in the figure, apparent resistivity increases with time, indicating conductive unconsolidated sediment and weathered material overlying more resistive bedrock.

A pseudosection of apparent resistivity versus logarithmic time for soundings MCTEM3, MCTEM4, and MCTEM5 is shown in figure 6b. As can be seen in the figure, the apparent resistivity changes laterally across the test site.

All TEM soundings at the test site exhibit a crossover in received voltage from positive to negative as measurement time increases. Figure 6c shows a linear plot of received data from sounding MCTEM3 showing this crossover occurring near the time associated with channel 10. This effect, noticed occasionally by other TEM investigators (J. Duncan McNeill, Geonics Ltd., oral communication, 1987), has been termed an IP-type effect. This crossover effect deviates from the normal positive decay that would be expected from a diffusion of current through conductive strata following current shutoff in the transmitter wire. Software developed to simulate normal electromagnetic scattering can not be used to model data exhibiting this effect.

The IP-type effect in these data is considered to be less significant in the early time channels based upon an analysis of the apparent resistivity curves in figure 6a. The steep rise in apparent resistivity at late-time is due to the plunging signal (dB/dt) near the crossover. A change in curvature in these curves after channel 6 suggests that early-time samples may be unaffected (or at least less affected) by the IP-type effect.

Based upon this analysis, channels 1-4 from sounding MCTEM1 were inverse modeled simultaneously with resistivity data from sounding MCVES7 in an effort to improve resolution of the geoelectric section. Computer programs CIPINV (John Groenewold, formerly with NJ. Geological Survey, written communication, 1987), and EINVRT (Stewart Sandberg, N. J. Geological Survey, written communication, 1988) which simultaneously invert resistivity/IP and resistivity/TEM data respectively, were used in tandem to create a single geoelectric model to fIt resistivity, IP, and TEM data from soundings MCVES7 and MCTEM1 with data fits shown in figures 5b and 6d. Note the rapid increase in TEM apparent resistivity as time increases; this could not be simulated in the modeling (fig. 6d). The interpreted depth to saprolite is the sum of modeled thicknesses of layers one, two, and. three which is 68 ft, with unweathered bedrock at 117 ft. These results compare very favorably

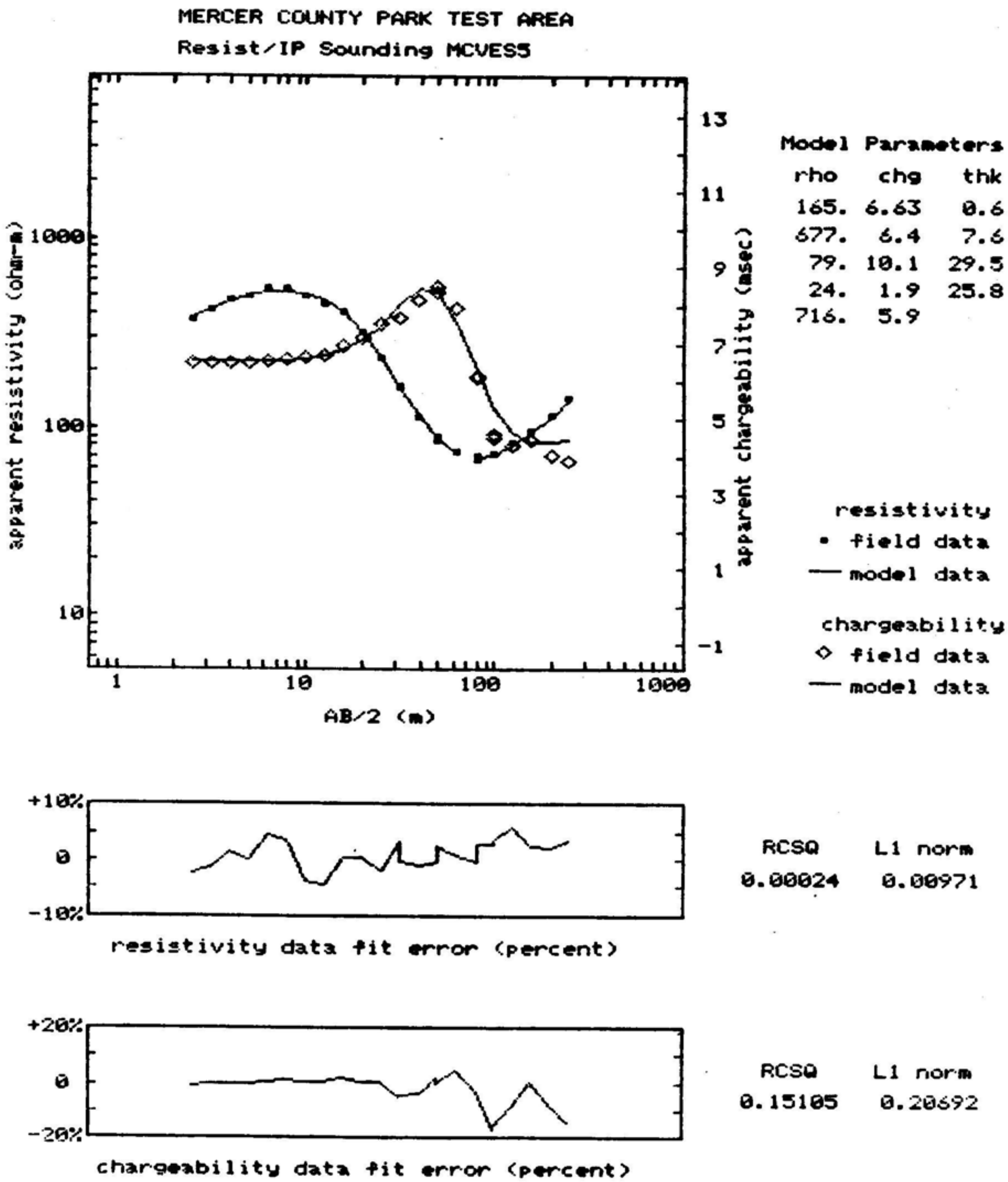

Figure 5a. Schlumberger sounding resistivity and induced polarization curves (MCVES 5) and interpretation.

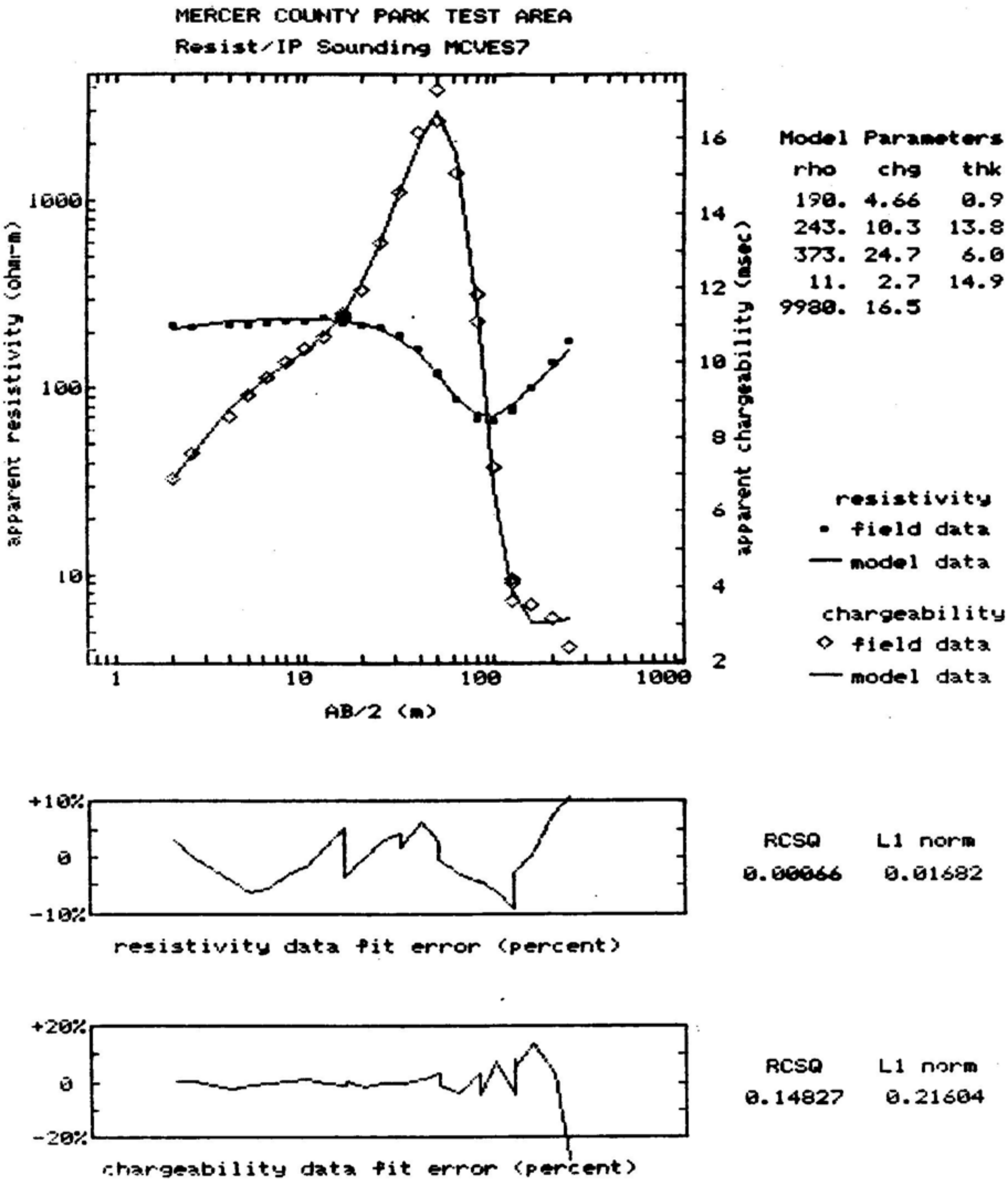

Figure 5b. Schlumberger sounding resistivity and induced polarization curves (MCVES 7) and interpretation.

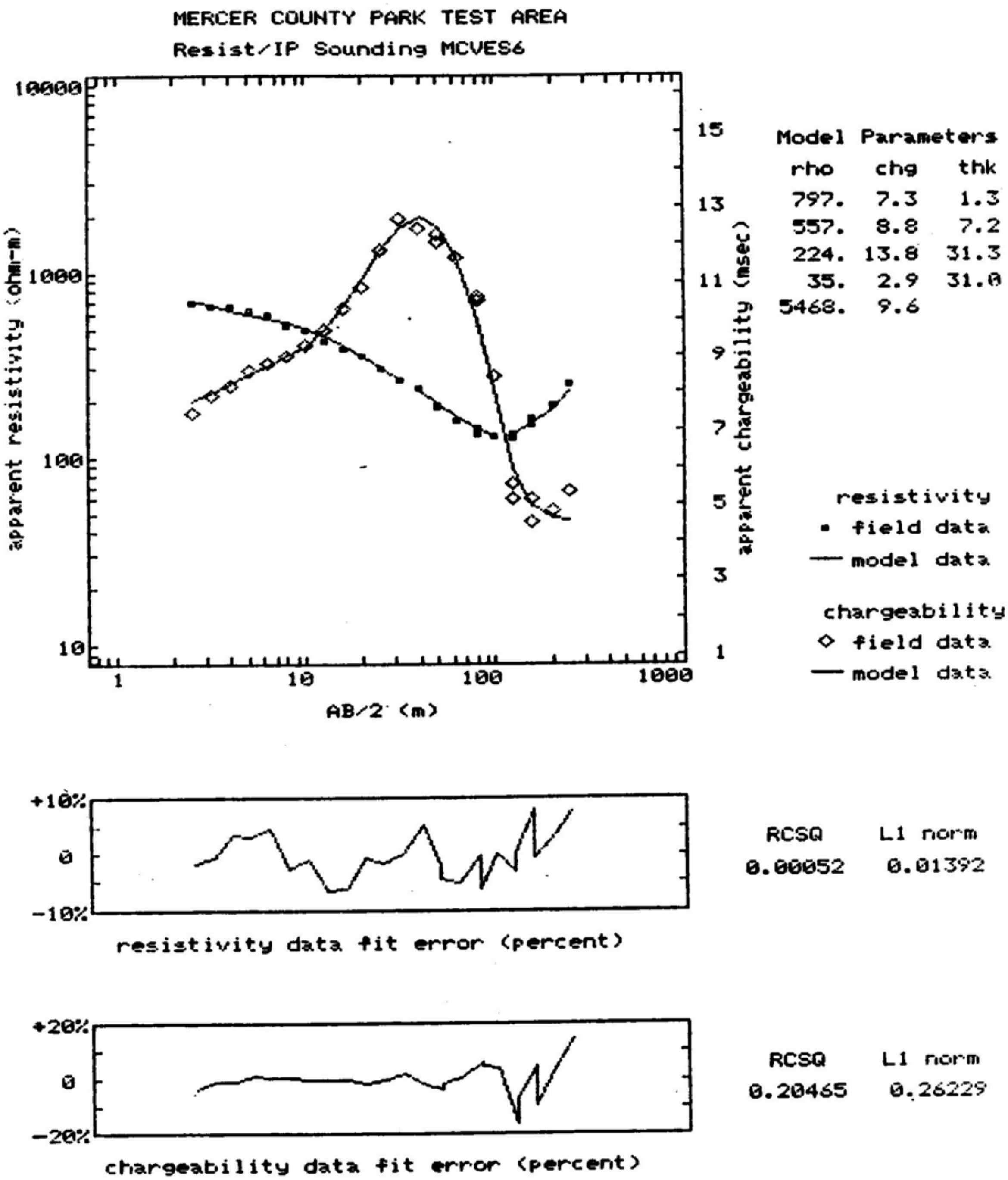

Figure 5c. Schlumberger sounding resistivity and induced polarization curves (MCVES 6) and interpretation.

Figure 6. a. Transient electromagnetic curves MCTEM 3, MCTEM 4 and MCTEM 5.

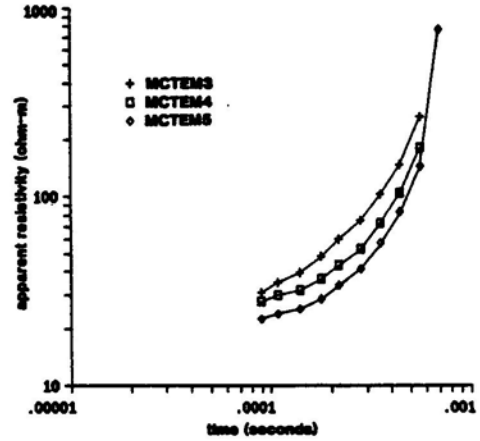

b. Pseudosection plot of TEM soundings MCTEM 3, MCTEM 4 and MCTEM 5.

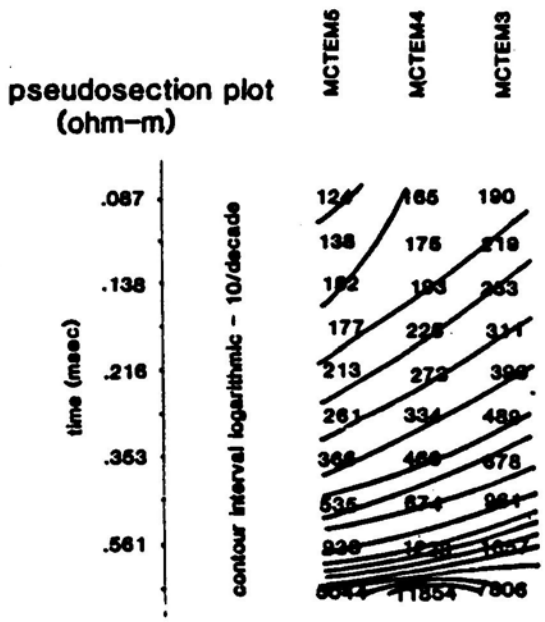

c. Linear plot of field data from TEM sounding MCTEM 3

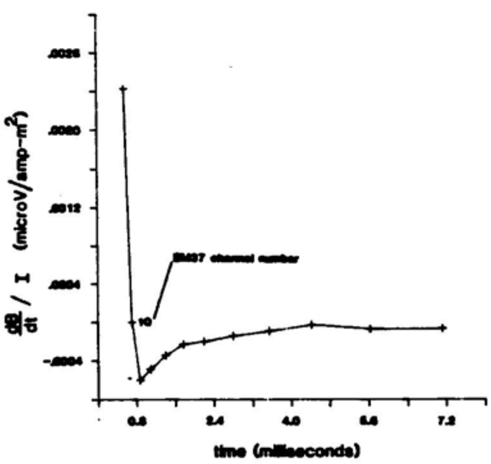

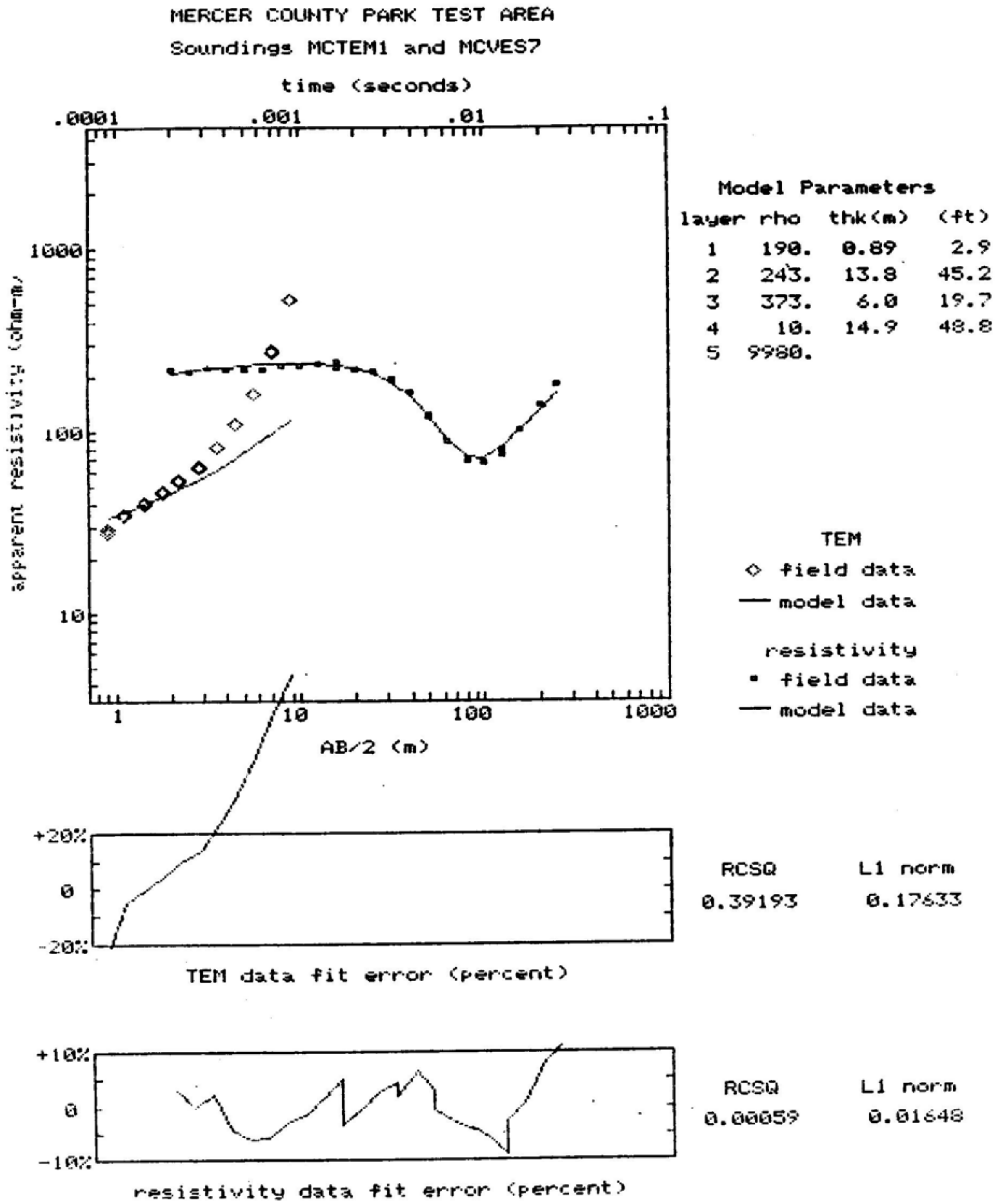

Figure 6d. Schlumberger resistivity sounding resistivity MCVES 7) with TEM sounding and interpretation.

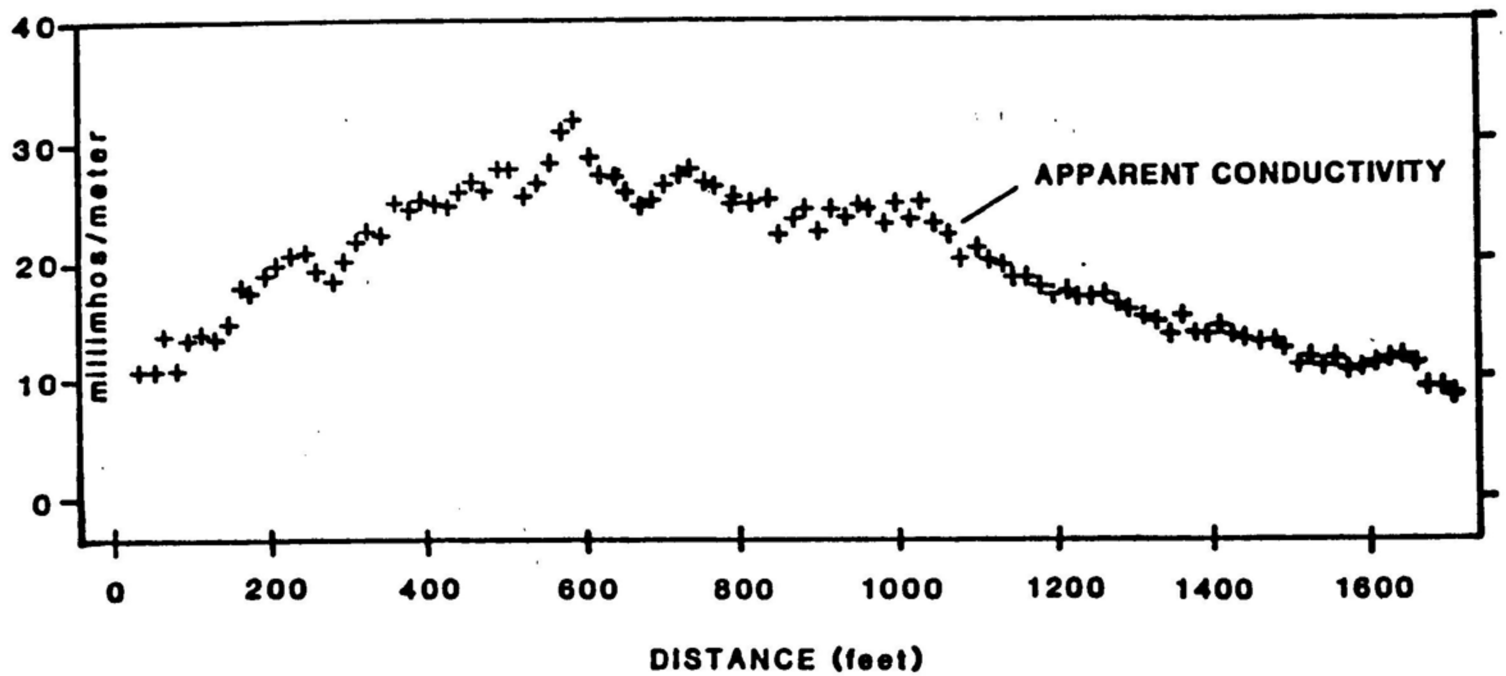

Figure 6e. Terrain-conductivity profile data.

with data from the nearby borehole (see section on borehole geophysics).

The use of TEM data with the inversion process improved resolution of saprolite thickness. This thickness was unresolvable using resistivity alone because of the well known thin~layer-equivalence problem. This same layer is probably too thick as modeled in soundings MCVES5 and MCVES6 (figs. 5a and 5c) since these thicknesses are not well resolved.

Terrain-conductivity measurements consisting of the apparent conductivity instrument readings (in millimhos per meter) are shown in profile form in figure 6e. Interpretation of terrain-conductivity data is usually qualitative and consists of contouring instrument readings acquired in a grid pattern. The resulting contour map usually corresponds to lateral resistivity contrasts associated with differing depths to the water table, or to conductive material intruded into homogeneous strata.

In this case, the terrain conductivity method is responding to both the thickness and resistivity of the unconsolidated sediment-and-saprolite zone (layers 1-4) in the resistivity-IP model. Note how the readings mimic the inverse of the bedrock surface in figure 4. This close relationship indicates that thickness is the primary influence, and that resistivity is secondary, even though it changes by more than a factor of two across the profile.

Microgravity

A gravity reduction program was used to calculate the simple Bouguer gravity anomalies according to formulas presented in Dobrin (1976). The gravity readings at each station were converted to observed gravity by first correcting for tidal and instrumental drift from base station readings repeated every hour. The latitude correction at each station was calculated using the secondary base station. as a reference. The theoretical sea-level gravity at each station was determined from the International Gravity Formula of 1930 (Dobrin, 1976).

The effect of elevation was determined from free-air and Bouguer reductions. A density of 2.67 g/cm^3 was used in the Bouguer correction. Terrain corrections were unnecessary because of the relatively flat topography of the area.

Depths to saturated sediment and bedrock obtained from seismic and resistivity- IP data were used to constrain depths in the gravity interpretations. These depths were used to calculate the initial model parameters for the two-dimensional gravity inversion program G2DINV (John Groenewold, formerly with N J. Geological Survey, written communication, 1986). This is a nonlinear, least-squares inversion program which incorporates the Marquardt procedure (Beck and Arnold, 1977).

G2DINV first fitted a linear regional to the simple Bouguer gravity values to give residual gravity anomalies (fig. 7). The residual gravity proftle closely coincided with layer four identified using seismic interpretation (fig. 4). The gravity field of the initial model was calculated using the Talwani algorithm (Talwani and others, 1959). The initial model included two bodies. The first body consisted of the two nearsurface layers (probably, based on seismic interpretation, unsaturated and saturated sand and gravel). It was assigned a density contrast of -0.85 g/cm^3 with the host rock. The second body, which represented the third layer, was assigned a density contrast of -0.35 g/cm^3. New parameters were calculated if the calculated gravity data did not adequately fit the observed data. After inverting on the density contrasts, the two bodies had density contrasts with the host rock of -0.94 g/cm^3 for the first body and -0.31g/cm^3 for the second body. The calculated model fit the observed model with a reduced chi squared error of 0.004 $mGal^2$. The most reasonable geological model was the one which coincided closely with the depths from the seismic model. The density contrasts were also reasonable for the rock types. Figure 7 shows the fmal gravity model.

Magnetics

The magnetic data were corrected to take into account the daily variations of the earth's magnetic field. The station readings were corrected by assuming a linear diurnal drift between base station readings. A constant was added to each segment between base readings to make all base station readings equivalent.

The total magnetic field anomaly was plotted in profile form (fig. 8). This profile shows a magnetic high of about 200 gammas near the western end of the proftle. The magnetic inversion program M2HINV (John Groenewold, formerly with NJ. Geological Survey, written communication, 1986) was used to model the data. This program uses the 2.5 dimensional al-

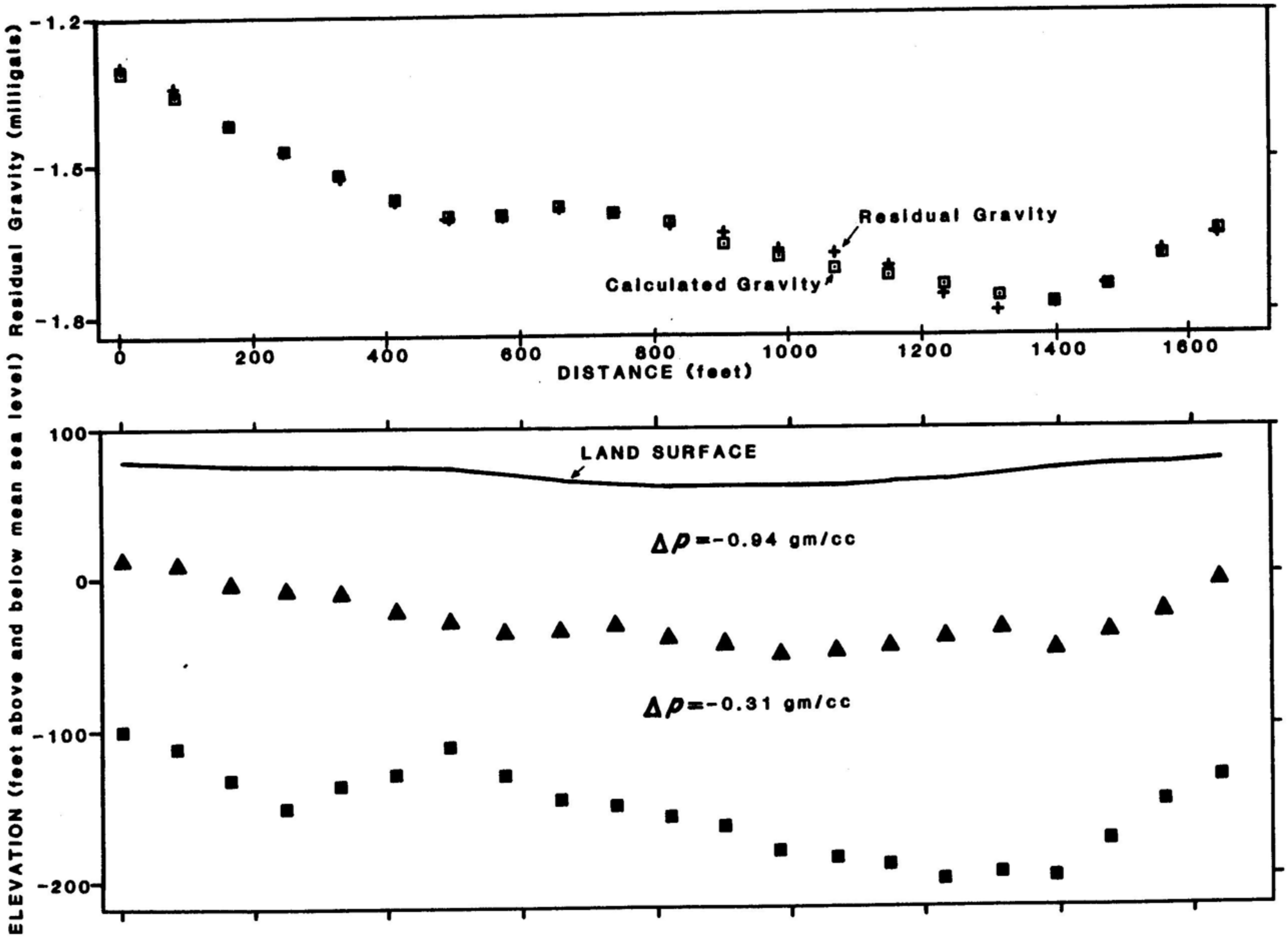

Figure 7. Residual gravity profile and interpretaive model, showing density contrasts.

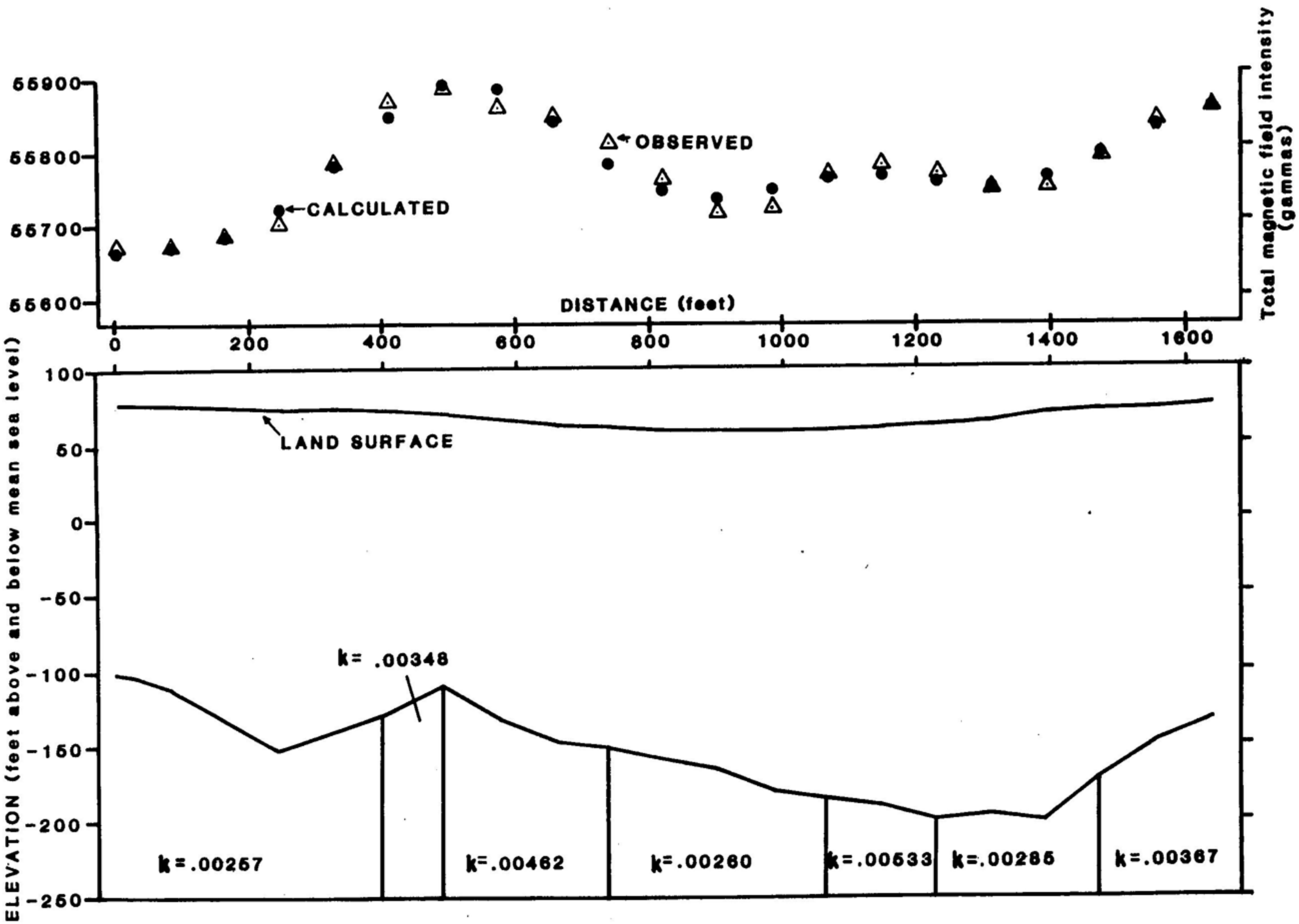

Figure 8. Total magnetic field intensity profile and interpretive model, showing modeled bodies and their associated magnetic susceptibilities.

gorithm of Shuey and Pasquale (1973) to calculate the magnetic field of the initial model. The program is non-linear, least-squares inversion software that incorporates the Marquardt procedure (Beck and Arnold, 1977).

The program first inverted for the regional using the third and fourth layer interface, as determined from the seismic interpretation, as top of the bedrock. The bedrock was subdivided into eight bodies of varying susceptibilities. The program then inverted for the susceptibilities. The calculated magnetic field from the model fit the observed magnetic data with a reduced chi squared error of 201.0 gammas^2 for the 21 stations. The calculated susceptibilities are similar to those in Fisher and others (1979) for the Wissahickon in this area. The calculated and total magnetic anomaly profiles, with the interpreted model, are shown in figure 8.

The Wissahickon Formation, believed to be bedrock in the study area (fig.2), locally contains large and small pods of gabbro and serpentine (Fisher and others, 1979). Some magnetic anomalies reflect the presence of these pods rather than higher susceptibilities within the schist itself. However, Fisher and others (1979) interpreted the regional pattern of magnetic anomalies to indicate refolded folds in units of differing magnetic susceptibilities. In this study, modeling using the inversion program indicated that the susceptibilities in bedrock differ locally. Whether this is due to refolding or to the presence of pods of gabbro and serpentine, is not known.

Borehole geophysics

The natural gamma log (fig. 9) shows a high natural gamma response in the interval from 18 ft to 28 ft below the surface. This is probably a clay layer in the unconsolidated sediments. This interpreted clay layer was not observable in the resistivity data from nearby sounding MCVES 7. The fluctuating, high response from 75 ft to 128 ft corresponds to a highly-weathered, clay-rich saprolite shown in the lithologic log (fig. 9). At 135 ft and 220 ft (fig. 9) there are peaks in the log which are probably due to high potassium content of the granite and alaskite. At depths of 138 ft to 215 ft the log is relatively flat with minor fluctuations attributable to small variations in the gneissic rock. Figure 9 also shows a depression in the log from 228 ft to 258 ft in the altered, chloritic, mafic zone. The natural gamma response increases below 258 ft to the depth of . drilling at 270 ft. A gneissic rock has been identified at those depths (fig. 9).

The single-point resistance log (fig. 9) fluctuates considerably due to the presence of fractures within the gneissic bedrock. These fractures may be water-bearing, causing a lower resistance at certain depths. The reason for the low resistance zone (trough) in the log from 215 ft to 228 ft has not been defmed. The alaskite rock observed at this depth is not fractured and no conductive minerals have been identified, but the rock appears to be more conductive than surrounding rock.

CONCLUSIONS

In the past, integrated geophysics has been applied primarily in petroleum and mineral exploration and most studies covered large areas. In general, integrated geophysical surveys have been found to be reliable and more cost effective than drilling.

In this study, we have used several geophysical techniques in a small area to determine the most effective combination of techniques to delineate the bedrock surface and interpret physical properties of the overlying sediments. The composite bedrock and overburden profile (fig. 10) shows the interpreted models from all the techniques used.

Seismic refraction proved successful in locating the water table and the bedrock surface. A limitation of this method is that field parameters such as geophone intervals or shotpoint offsets have to be selected so as to obtain optimum data from near-surface as well as deeper layers. This limitation is a hinderance especially when profiling in a small area. In this study, the upper, weathered portion of the bedrock (saprolite) was not resolved from the unconsolidated sediments. Nor were the thin alaskite and granitic layers resolvable because the velocity contrasts between these layers and the gneissic bedrock were insignificant. The top of the altered mafic rock, which has a higher velocity than the gneiss, was well resolved.

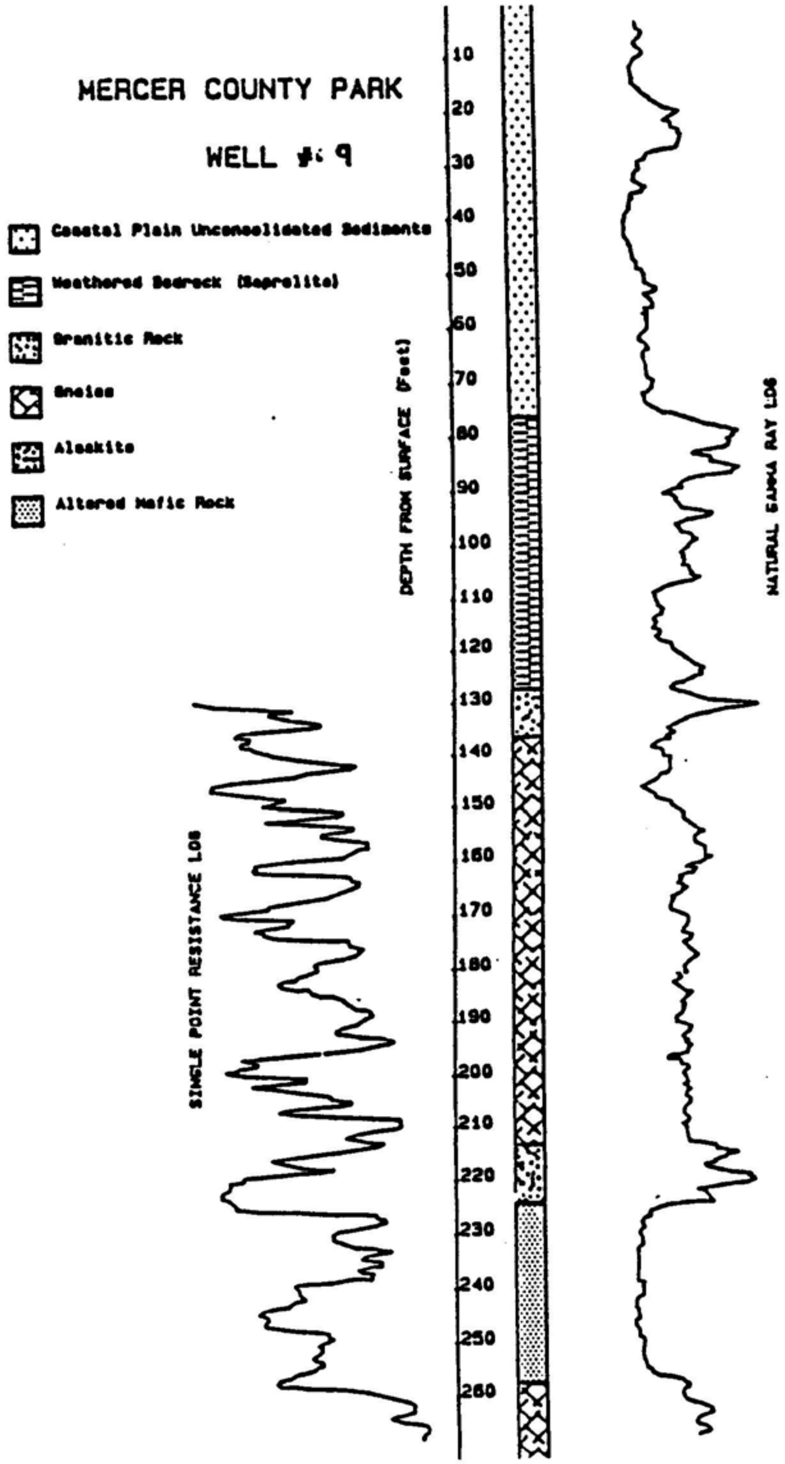

Figure 9. Natural gamma log, single-point resistance log and borehole lithologic log.

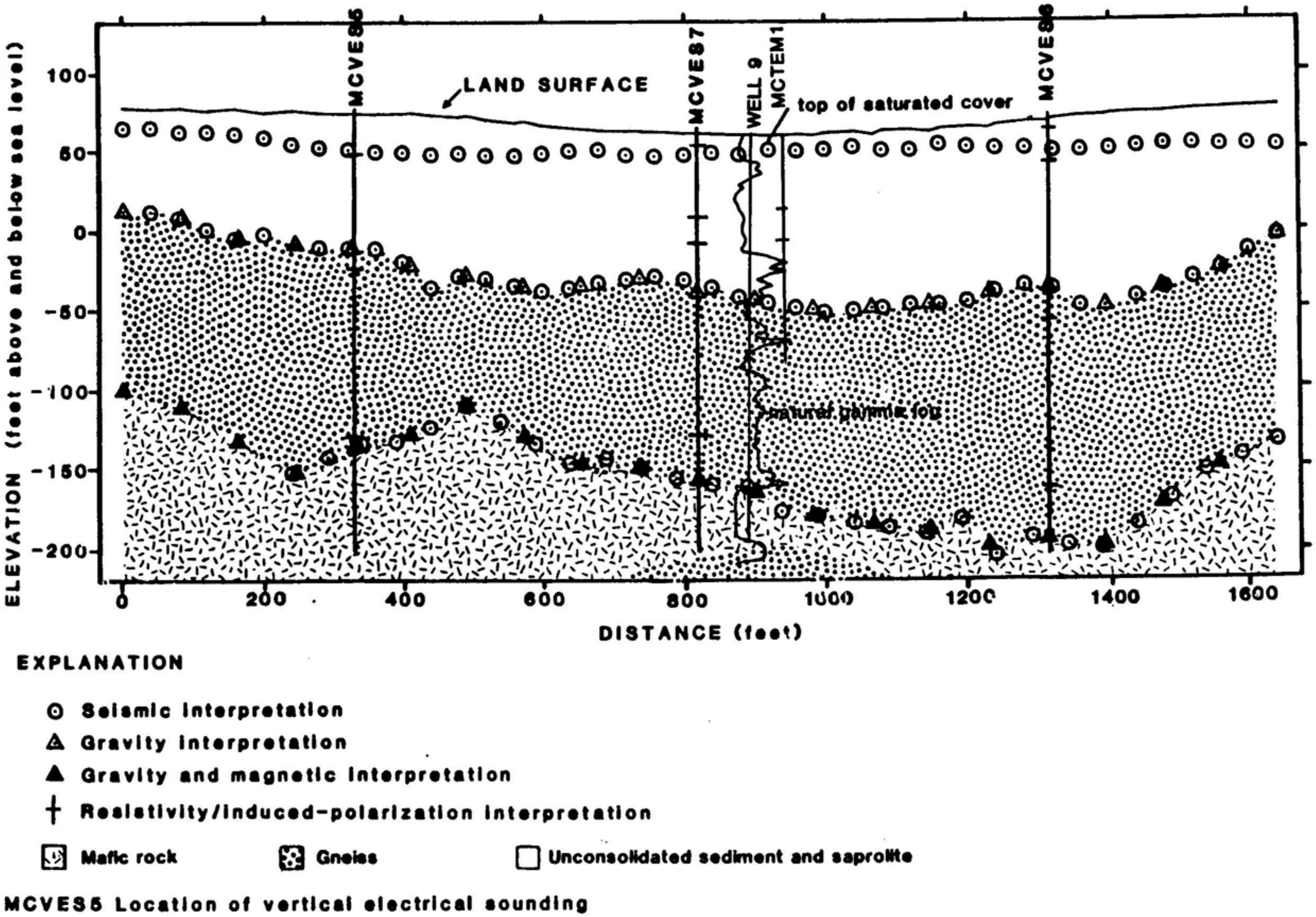

Figure 10. Composite bedrock and overburden profile.

The electrical-resistivity/induced-polarization soundings effectively resolved near-surface layers. An increase in modeled chargeability at depth in the overburden, indicating increasing clay or silt and a definable depth to the top of the saprolite were the significant results.

The transient electromagnetic (TEM) sounding and terrain conductivity methods both showed a minor lateral resistivity change across the site. Simultaneous TEM and resistivity modeling resulted in an accurate saprolite thickness as compared to a nearby borehole. However, an IP-type effect in the TEM data rendered all but the fIrst few time samples unusable.

Ambiguity in gravity interpretation was resolved by constraining depths of geologic units to those of layers identified by seismic refraction. Through inverse modeling, densities were determined which proved to be reasonable for the geologic setting. Thus, the gravity method proved to be successful when used in conjunction with the seismic refraction method. One drawback is that microgravity surveys require knowledge of surface elevations to within a couple of inches to detect minor anomalies. This may not be cost-effective or practical in surveys of large areas.

The interpretation of magnetic data can also be ambiguous. In this study the depths were constrained using seismic refraction data. Knowledge of the magnetic susceptibilities of the local rocks is necessary for meaningful results. In the present study the susceptibility of the bedrock seemed to vary within short distances.

The natural gamma borehole log corresponded to variations shown on the lithologic log. No core was collected in the unconsolidated-sediments layer to defInitely distinguish the lithology corresponding to the high gamma count. The single-point resistance log was strongly affected by fractures and water within the fractures.

This study demonstrates that for delineation of the saturated zone and bedrock surface and determination of lithology, a combination of two or more geophysical methods is much more powerful than the same methods applied singly

REFERENCES

Beck, J. w., and Arnold, K. J., 1977, Parameter estimation in engineering and science: New York, John Wiley, 501 p.

Bonini, W. E., and Woollard, G. P., 1957, Observational accuracy of high-range geodetic type Worden gravimeters: American Geophysical Union Transactions, v. 38, p. 147-155.

Dobrin, M. B., 1976, Introduction to geophysical prospecting, 3rd ed.: New York, McGrawHill, 630 p.

Eaton,' G. P., and Watkins, J.S., 1970, The use of seismic refraction and gravity methods in hydrogeological investigations: in Morley, L. W., ed., Mining and Ground Water Geophysics: Geological Survey Canada Economic Geology Report 26, p. 544-568.

Fisher, G. w., Higgins, M. w., and Zietz, Isidore, 1979, Geological interpretations of aeromagnetic maps of the crystalline rocks in the Appalachians, N. VU'ginia to New Jersey: Maryland Geological Survey, Report of Investigations no. 32, 43 p.

Hoffman, J. L. and Waldner, J. *S.*, 1985, HRASSD: High Resolution Analysis of Shallow Seismic Data, New Jersey Geological Survey Open-file Report 86-1, 74 p.

Johnson, M.E., 1950, Geologic map of New Jersey: New Jersey Geological Survey State Atlas, sheet 40, scale 1:250,000.

Koefoed, 0., 1972, Computation of type curves for electromagnetics: Geophysical Prosp., v. 20, p. 406.

Lennox, D. H., and Carlson, v., 1967, Geophysical exploration for buried valleys in an area north of Two Hills, Alberta: Geophysics, v. 32, p. 331-362.

van Overmeeren, R. A., 1981, A combination of electrical resistivity, seismic refraction, and gravity measurements for ground water exploration in Sudan: Geophysics, v. 46, p. 1304-1313.

Sandberg, S. K., 1988, Microcomputer software for the processing and forward modeling of transient electromagnetic data taken in the central loop sounding configuration: New Jersey Geological Survey Open-me Report 88-1.

Scott, J. H., 1977, SIPT-A seismic refraction inverse modeling program for timeshare terminal computer systems: U.S. Geol. Surv. Open-file Report 77-365.

Scott,J. H., Tibbetts B. L., and Bordick, B. G., 1972, Computer analysis of seismic refraction data: Bureau of Mines Report of Investigations RI-7595.

Shuey, R. T., and Pasquale, A. *S.*, 1973, End corrections in magnetic proftle interpretation: Geophysics, v. 28, p. 507-512.

Talwani, Manik, Worzel J. L., and Landisman, M., 1959, Rapid gravity computations for two-dimensional bodies with application to the Mendocino submarine fracture zones: Journal Geophysical Research, v. 64, p. 4959.

Telford, W. M., Geldart, L. P., Sheriff, R. E., and Keys, D. A., 1976, Applied Geophysics: Cambridge, England: Cambridge University Press, P 859.

U.S. Geological Survey, 1979, Aeromagnetic map of parts of Delaware and New Jersey: Open File Report 79-1683.

Widmer, Kemble, 1965, Geology of the ground water resources of Mercer County: New Jersey Geological Survey Geologic Report Series 7.

APPENDIX

Well records

Well no.	Permit no.	Surface elevation in feet above sea level	Bedrock elevation in feet above sea level
1	28-6008	110	-117
2	28-12344	70	-43
3	28-4621	84	40
4	28-3541	80	-20
5	28-4013	70	20
6	28-856	80	-8
7	28-1961	80	10
8	28-15613	100	8
9	28-17436	63	-15

DETERMINATION OF BEDROCK TOPOGRAPHY AND GEOLOGY USING VARIOUS GEOPHYSICAL TECHNIQUES
(New Jersey Geological Survey Technical Memoradum TM 89-2)